

Article

Spatial Forecasting of Dissolved Oxygen Concentration in the Eastern Black Sea Basin, Turkey

Sinan Nacar ¹, Adem Bayram ¹, Osman Tugrul Baki ², Murat Kankal ^{3,*} and Egemen Aras ⁴

¹ Civil Engineering Department, Engineering Faculty, Karadeniz Technical University, Trabzon 61080, Turkey; sinannacar@hotmail.com (S.N.); adembayram@gmail.com (A.B.)

² Civil Engineering Department, Technology Faculty, Karadeniz Technical University, Trabzon 61830, Turkey; tugrul92@gmail.com

³ Civil Engineering Department, Engineering Faculty, Bursa Uludağ University, Bursa 16059, Turkey

⁴ Civil Engineering Department, Engineering and Natural Sciences Faculty, Bursa Technical University, Bursa 16310, Turkey; egemen.aras@btu.edu.tr

* Correspondence: mkankal06@gmail.com; Tel.: +90-5325625933

Received: 7 February 2020; Accepted: 24 March 2020; Published: 7 April 2020



Abstract: The aim of this study was to model, as well as monitor and assess the surface water quality in the Eastern Black Sea (EBS) Basin stream, Turkey. The water-quality indicators monitored monthly for the seven streams were water temperature (WT), pH, total dissolved solids (TDS), and electrical conductivity (EC), as well as luminescent dissolved oxygen (LDO) concentration and saturation. Based on an 18-month data monitoring, the surface water quality variation was spatially and temporally evaluated with reference to the Turkish Surface Water Quality Regulation. First, the teaching–learning based optimization (TLBO) algorithm and conventional regression analysis (CRA) were applied to three different regression forms, i.e., exponential, power, and linear functions, to predict LDO concentrations. Then, the multivariate adaptive regression splines (MARS) method was employed and three performance measures, namely, mean absolute error (MAE), root means square error (RMSE), and Nash Sutcliffe coefficient of efficiency (NSCE) were used to evaluate the performances of the MARS, TLBO, and CRA methods. The monitoring results revealed that all streams showed the same trend in that lower WT values in the winter months resulted in higher LDO concentrations, while higher WT values in summer led to lower LDO concentrations. Similarly, autumn, which presented the higher TDS concentrations brought about higher EC values, while spring, which presented the lower TDS concentrations gave rise to lower EC values. It was concluded that the water quality of the streams in the EBS basin was high-quality water in terms of the parameters monitored in situ, of which the LDO concentration varied from 9.13 to 10.12 mg/L in summer and from 12.31 to 13.26 mg/L in winter. When the prediction accuracies of the three models were compared, it was seen that the MARS method provided more successful results than the other methods. The results of the TLBO and the CRA methods were very close to each other. The RMSE, MAE, and NSCE values were 0.2599 mg/L, 0.2125 mg/L, and 0.9645, respectively, for the best MARS model, while these values were 0.4167 mg/L, 0.3068 mg/L, and 0.9086, respectively, for the best TLBO and CRA models. In general, the LDO concentration could be successfully predicted using the MARS method with various input combinations of WT, EC, and pH variables.

Keywords: dissolved oxygen; Eastern Black Sea Basin; multivariate adaptive regression splines; stream water quality; teaching–learning based optimization

1. Introduction

Water quality management plays the most important role in the control of surface water pollution and the planning of river basins. The possible pollution of clean water resources by industrial and

municipal wastes has always been a concern for users of these water resources. Dissolved oxygen (DO) concentration, which is one of the main indicators in determining the quality of surface waters, has received great attention in the literature in recent years [1]. The major sources of DO are (i) reaeration from the atmosphere, (ii) enhanced aeration at weirs and other structures, (iii) photosynthetic oxygen production, and (iv) the introduction of DO from other sources, such as tributaries [2,3].

The DO concentration used in the determination of the quality of surface waters is significantly affected by the physical, chemical, and biological factors of the river and combinations of these factors [3–6], and has both a seasonal and a daily cycle [7]. DO concentration in surface waters is a water quality parameter that is significantly affected by temperature. The solubility of oxygen in water decreases as the water temperature (WT) increases. Based on this relationship, it is possible to say that cold water holds more DO than hot water. DO concentration is high in winter and spring months when the WT is low, while DO concentration in water is low in summer and autumn months when the WT increases. When making pH measurements, it is important to take into account the temperature parameter, which has an important effect on hydrogen-ion activities. DO concentration is also dependent on the electrical conductivity (EC). Low WT as well as low conductivity and high atmospheric pressure are the factors that increase DO concentration in water [8]. Therefore, DO, WT, EC, and pH, which are monitored by many researchers [9–12] are important water-quality indicators.

Measurement of DO concentration or saturation in the rivers is very important for the determination of the quality of rivers and water resources management. Although it is difficult to constantly monitor the change in DO concentration, much effort is being made to establish models that determine this change based on other water-quality indicators. This is the main motivation for studies to predict DO concentration using other water-quality indicators [2,13,14]. Various methods have been used in the simulation and prediction of DO in surface waters. Some of them are artificial neural networks [15,16], Mike 11 [17], adaptive neuro-fuzzy inference system [18,19], etc. Among them, multivariate statistical techniques have been widely used to characterize water quality [20–24].

The surface water quality has been monitored by the 22nd Regional Directorate of State Hydraulic Works in the Eastern Black Sea (EBS) Basin, Turkey. However, the monitoring studies are spatially and temporally limited since it is expensive to set up water quality monitoring stations at desired locations. Spatially, the streams Yomra and Manahoz from the basin, for example, have not been monitored. Temporally, the monitoring frequency is quarterly for the streams Foldere, Kalenima, Karadere, and Solaklı from the basin. Moreover, the surface water quality data have not been published. On the other hand, the researchers from Turkish universities have been closely interested in the surface water quality in the basin. Gultekin et al. [10] monitored and assessed the water quality for a lot of streams in the basin but for a limited duration, spring of 2009. Bayram [11] monitored and assessed the water quality for Değirmendere Stream only from the spring of 2010 to the winter of 2011. Koralay et al. [12] monitored and assessed the water quality for the Solaklı Stream, only from January to December 2014.

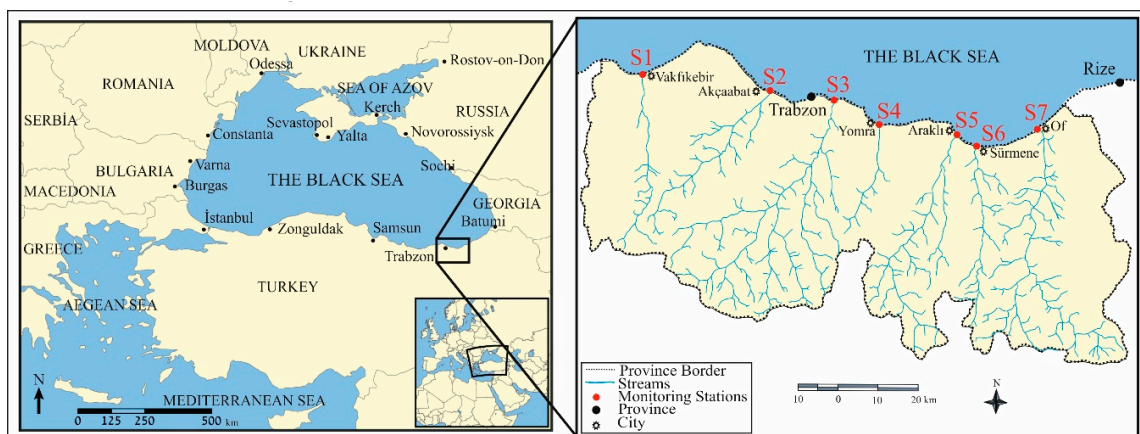
The two main objectives of this study are (i) to monitor and assess the water quality of the aforementioned streams, as well as the Değirmendere Stream, in terms of WT, pH, luminescent dissolved oxygen (LDO) concentration and saturation, total dissolved solids (TDS), and EC, and (ii) to predict the stream LDO concentration by developing appropriate equations by way of the multivariate adaptive regression splines (MARS), teaching–learning based optimization (TLBO), and conventional regression analysis (CRA) methods. The stream WT, EC, and pH were selected as input variables. Various combinations of these variables were used for modeling LDO concentration. Predictions from all methods were also compared with each other. To the authors' knowledge, there has not been any published study that compared the MARS, TLBO, and CRA methods in modeling LDO concentrations.

The paper is structured into four sections. The information about the study area, modeling variables, the techniques used for modeling and the model development applications are introduced in the next section. Then, the water quality monitoring and LDO modeling results are presented in the third section. The summary and some conclusions are then made in the final section of the paper.

2. Materials and Methods

2.1. Study Area

There are 25 hydrological basins in Turkey. With a mean annual surface water potential of $16.46 \times 10^9 \text{ m}^3$ in 2016 [25], the EBS basin is of prime importance, in comparison with a mean annual groundwater potential of $0.49 \times 10^9 \text{ m}^3$ in 2016. The EBS basin comprises the provinces Ordu, Giresun, Trabzon, and Rize, respectively, along the Southeastern Black Sea coast. The Trabzon Province with a total population of 779,379, according to the 2016 census [26] is the biggest city in the basin. There are a lot of streams draining the major agricultural, urban, and industrial areas of the Trabzon Province, where sanitary sewage systems serve 623,503 people, according to the municipal wastewater statistics survey in 2016 [27]. About $73.966 \times 10^6 \text{ m}^3$ per year of wastewater are generated, $3.111 \times 10^6 \text{ m}^3$ of which discharge through the streams to the Black Sea [27]. As a result of this discharge, the stream water quality might be affected negatively. For this reason, the streams that are vital for the province, where the groundwater potential is insignificant, were selected for the water quality monitoring. Considering the modeling studies at a later stage, it was also decided to monitor seven streams, three of which were to the west and three of which were to the east, with reference to the Yomra Stream located in the middle part of the province. In this way, it was possible to represent the study area completely. The streams monitored from west to east were the Foldere, Kalenima, Değirmendere, Yomra, Karadere, Manahoz, and Solaklı, respectively. One monitoring station, where the stream discharges into the Black Sea, was selected for each stream along the coast of Trabzon Province in the basin (Figure 1).



S1: 41°02'48.69" N - 39°16'40.22" E S2: 41°01'07.80" N - 39°35'46.20" E S3: 41°00'06.00" N - 39°45'25.80" E S4: 40°57'10.80" N - 39°52'03.00" E
S5: 40°56'05.40" N - 40°03'38.40" E S6: 40°54'52.80" N - 40°06'41.40" E S7: 40°56'35.40" N - 40°16'01.80" E

Figure 1. The stream water-quality monitoring stations selected in the Eastern Black Sea Basin, Turkey.

2.2. The Stream Gauging

There are a lot of stream gauging stations in the basin, however, many of which are not operational for various reasons. Therefore, it can be asserted that the coastal part of the Trabzon Province is poorly gauged. Nevertheless, there were seven stream gauging stations operated by the 22nd Regional Directorate of General Directorate of State Hydraulic Works in the study area. However, the flow rate data recorded from four stations—the Şerifli station on the Foldere Stream, the Öğütlü station on the Değirmendere Stream, the Taşdelen station on the Yomra Stream, and the Ağnas station on the Karadere Stream, respectively, during the study period (March 2015–August 2016). The characteristics of these stations are given in Table 1 [28].

Table 1. Location features of the stream gauging stations operated in the study area.

Stream	Gauging Station	Coordinates	Drainage Area (km ²)	Operating Altitude (m)	Gauging (2015–2016)
Foldere	Şerifli	39°17'06" E – 41°00'59" N	181.30	60	Yes
Kalenima	Doğanköy	39°28'10" E – 40°54'10" N	129.40	410	No
Değirmendere	Öğütlü	41°11'00" E – 40°51'50" N	728.40	160	Yes
Yomra	Taşdelen	39°51'23" E – 40°51'14" N	68.85	385	Yes
Karadere	Ağnas	40°00'25" E – 40°50'58" N	635.70	78	Yes
Manahoz	Ortaköy	40°07'00" E – 40°51'00" N	174.00	150	No
Solaklı	Ulucami	40°15'20" E – 40°45'00" N	576.80	275	No

2.3. Stream Water Quality Monitoring

We employed two Hach HQ40d portable multi-parameter meters to monitor the stream DO concentration (mg/L) and saturation (%), pH and TDS (mg/L), and EC ($\mu\text{s}/\text{cm}$), simultaneously, since the Hach HQ40d portable multi-parameter meter had only two input channels for simultaneous measurement. The first one was equipped with the conductivity probe (CDC401) and a pH electrode (PHC101), and the second one was equipped with the Luminescent/Optical DO probe (LDO101). The stream WT could be measured by the LDO probe, as well as the pH electrode and the conductivity probe. The stream WT, pH, LDO concentration and saturation, TDS, and EC were automatically measured and recorded in situ for 15 min, at 30 s intervals. The final result was presented as the arithmetic mean of the 30 readings. All measurements were conducted monthly at seven monitoring stations during the study period (March 2015–August 2016).

2.4. Modeling Variables

In water quality modeling studies, determining the independent variables was the most important part of the study. Therefore, the independent variables must be chosen appropriately. By considering the literature about DO modeling, a wide variety of water quality variables were used (Table 2). These variables were flow rate (Q), WT, pH, EC, specific conductivity (SC), water depth (WD), total solids (TS), total alkalinity (TA), water hardness (WH), air temperature (AT), nitrite ion (NO_2^-), nitrate ion (NO_3^-), ammonium ion (NH_4^+), phosphate ion (PO_4^{3-}), total phosphorus (TP), chemical oxygen demand (COD), sulfate ion (SO_4^{2-}), sodium ion (Na^+), potassium ion (K^+), calcium ion (Ca^{2+}), chloride ion (Cl^-), and biochemical oxygen demand (BOD). Taking into account the literature review [29–48], the WT, the EC, and the pH (which are most effective in modeling studies) were selected as the independent variables.

2.5. Multivariate Adaptive Regression Splines (MARS) Method

The MARS method is a non-parametric, flexible, and rapid regression method, first presented by Friedman [49]. It does not presuppose the functional relationships between input and output variables used in modeling [50,51]. Instead, it attempts to determine the relationship between variables by dividing the data into subsets of data. With this process, the training data set was divided into linear segments called splines. The endpoints of these splines are called knots. Partial curves formed between the two knots are called basic functions [52]. This strategy made the MARS method more advantageous and flexible than the other statistical methods in multivariate modeling studies [53]. More details about the MARS and its implementation can be found in [54–56].

2.6. Teaching–Learning Based Optimization (TLBO) Algorithm

The TLBO algorithm is a meta-heuristic optimization algorithm developed by [57]. This algorithm is based on the phenomenon of teaching and learning. The TLBO algorithm has some advantages over other population algorithms. One of the most important advantages of the TLBO is that it does not require any parameters setting for the working of the algorithm, making the implementation of TLBO simpler [58]. More detailed information about the TLBO algorithm can be found in the literature [58–60].

2.7. Model Development Applications

The estimation and forecasting of the major parameters of surface waters are typically performed using various types of artificial intelligence–based techniques that rely on machine learning. This requires training, validation (the latter can be omitted if data are scarce) and test sets [61]. The process of separating data into training, validation, and test data sets can be done in a variety of ways. Csabragi et al. [61] evaluated the process of separating the data into training, validation, and test data sets under three headings. These are as follows—(i) random creation of the respective sets, (ii) assigning the majority of sampling points to the training set and a smaller proportion of sampling points to the test set, and (iii) assigning multiple initial years to the training set and a couple of final years to the test set. In this study, the data were divided into the training and test data sets, taking into account situation (ii). There were a total of 126 measurements, 90 of which were used for training (five streams) and the remaining measurements were reserved for testing (two streams). In this way, the method that gave the best results for the training dataset was tested for whether it gave good results for any stream in the EBS basin. Table 3 shows the division of streams as training and test groups.

Table 3. The division of the Eastern Black Sea (EBS) Basin streams used in the luminescent dissolved oxygen (LDO) modeling.

Stream	Training Group	Testing Group
Foldere	•	
Kalenima	•	
Değirmendere		▲
Yomra	•	
Karadere	•	
Manahoz		▲
Solaklı	•	

Note: Black circles for training group and black triangles for testing group.

The general approach to choose a good training data set from the available data is to include all extreme data in the training data set [62]. The minimum (Min), mean, maximum (Max), and standard deviation (SD) values for the water-quality indicators, which were employed for the training and testing data sets, are given in Table 4.

Table 4. Basic statistics for the water-quality indicators employed in the training and testing data sets.

Water-Quality Indicators	Training Data Set				Testing Data Set			
	Min	Mean	Max	SD	Min	Mean	Max	SD
LDO, mg/L	8.25	10.89	15.08	1.38	8.98	11.08	13.97	1.20
WT, °C	0.93	14.16	27.35	6.37	3.30	13.43	23.70	5.53
pH	7.62	8.37	9.68	0.37	7.41	8.26	8.98	0.37
EC, µS/cm	58.11	165.34	792.53	108.42	55.71	125.97	280.60	57.43

In the present study, different input combinations were established to determine the effect of the input variables on the LDO concentration. The input combinations created in the study were WT

(Model 1); WT and EC (Model 2); WT and pH (Model 3); and WT, EC, and pH (Model 4), respectively. Following the input combination and modeling process, the MARS method was applied to identify the equations that produced the results closest to the measured LDO concentration, by using the Salford Predictive Modeler 8.0 software. Then, three different regression functions, i.e., exponential, power, and linear, were used for the TLBO and CRA methods, which were chosen to optimize the unknown coefficients (w_i) of the independent variables (x_i) [52]. The equations of exponential, power, and linear functions are given below;

$$y_{Exponential} = w_0 + \exp(w_1 + w_2x_1 + w_3x_2 + \dots + w_{n+1}x_n) \quad (1)$$

$$y_{Power} = w_0x_1^{w_1}x_2^{w_2}x_3^{w_3}x_4^{w_4} \dots x_n^{w_n} \quad (2)$$

$$y_{Linear} = w_0 + w_1x_1 + w_2x_2 + w_3x_3 + \dots + w_nx_n \quad (3)$$

The optimization of the extreme values that can be found in the data set can be difficult. To facilitate optimization, minimize the impact of different dimensions, and achieve more effective results, all three input variables and the LDO were normalized using Equation (4) [63–65]. Different normalization formulas are also used in water quality modeling studies but there are no fixed rules as to which standardization approach should be used in particular circumstances [19,66]. In this study, “a” and “b” were taken as 0.8 and 0.1, respectively.

$$\text{Normalized value} = \left[\frac{\text{Raw value} - \text{Min value}}{\text{Max value} - \text{Min value}} \right] \times (a) + b \quad (4)$$

In the prediction of the LDO concentration, the aim was to determine the best model for obtaining the monitored values. In this context, three performance measures, i.e., root mean square error (RMSE), mean absolute error (MAE), and Nash Sutcliffe coefficient of efficiency (NSCE), were selected to assess the fitting accuracy and predictability of the MARS, TLBO, and CRA methods. The models with the highest NSCE values, as well as the lowest RMSE and MAE values had more accurate estimates than the other models [67,68]. The RMSE, MAE, and NSCE were calculated as follows:

$$\text{RMSE} = \sqrt{\frac{1}{N} \sum_{i=1}^N (t_i - td_i)^2} \quad (5)$$

$$\text{MAE} = \frac{1}{N} \sum_{i=1}^N |t_i - td_i| \quad (6)$$

$$\text{NSCE} = 1 - \frac{\sum_{i=1}^N (t_i - td_i)^2}{\sum_{i=1}^N (t_i - \bar{t})^2} \quad (7)$$

where t_i is the monitored value, \bar{t} is the mean of monitored values, td_i is the predicted value, and N is the total number of monitored values [52]. The TLBO algorithm parameters were used for the same values for all functions employed in the study. The number of iterations was 1000, the population size was 50, and the unknown coefficients in the regression equations were used in the range (−5, 5).

3. Results and Discussion

3.1. Stream Water-Quality Assessment

The legal documents related to water quality or water pollution in Turkey are published and amended from time to time, such as Turkish Water Pollution Control Regulation (TWPCR) [69], which

comprises quality classifications and are intended for the purposes of aquatic environments. It was published in the official gazette dated 31 December 2004 and numbered 25687. The Article 7, i.e., the intra-continental water resources classification, in the TWPCR [69] was employed by Turkish researchers, who engaged in surface water quality [24,70,71], for a long time. However, Turkish Superficial Water Quality Management Regulation (TSWQMR) was published in the official gazette dated 30 November 2012 and numbered 28483. Several articles, including Article 7, were repealed from the TWPCR [69] based on the Article 21 in the TSWQMR [72]. Moreover, a regulation about the first amendment for the TSWQMR [72] was published in the official gazette dated 15 April 2015, number 29327, and the name of the above-mentioned regulation was amended as Turkish Surface Water Quality Regulation [73]. The second amendment for the TSWQMR [72] was also published in the official gazette dated 10 August 2016, number 29797 [74]. Table 5 shows the upper threshold values [69,72,73,75] in terms of the monitored water-quality indicators.

Table 5. The comparison of Article 7 from TWPCR [69] with Article 21 from TSWQMR [72], Article 7 from TSWQR [73], and Article 7 from TSWQR [75], respectively, for the intra-continental surface water resources classification.

Water-Quality Indicators	Water Quality Classes, TWPCR [69]				Water Quality Classes, TSWQMR [72]			
	I	II	III	IV	I	II	III	IV
WT, °C	25	25	30	>30	≤25	≤25	≤30	>30
pH	6.5–8.5	6.5–8.5	6.0–9.0	<6.0 to >9.0	6.5–8.5	6.5–8.5	6.0–9.0	<6.0 to >9.0
DO, mg/L	8	6	3	<3	>8	6–8	3–6	<3
DO, %	90	70	40	<40	90	70–90	40–70	<40
TDS, mg/L	500	1500	5000	>5000	–	–	–	–
EC, µS/cm	–	–	–	–	<400	400–1000	1001–3000	>3000
Water-Quality Indicators	Water Quality Classes, TSWQR [73]				Water Quality Classes, TSWQR [75]			
	I	II	III	IV	I	II	III	IV
WT, °C	≤25	≤25	≤30	>30	–	–	–	–
pH	6.5–8.5	6.5–8.5	6.0–9.0	<6.0 to >9.0	6–9	6–9	6–9	6–9
DO, mg/L	>8	6	3	<3	>8	6	3	<3
DO, %	>90	70	40	<40	–	–	–	–
TDS, mg/L	–	–	–	–	–	–	–	–
EC, µS/cm	<400	1000	3000	>3000	<400	1000	3000	>3000

I: High-quality water, II: Slightly polluted water, III: Polluted water, and IV: Highly polluted water.

Taking into account a one-year period from March 2015 to February 2016 and a one-year period from September 2015 to August 2016, Table 6 gives the basic statistics of the water-quality indicators monitored for the surface waters from the EBS basin streams, namely the Foldere (S1), Kalenima (S2), Değirmendere (S3), Yomra (S4), Karadere (S5), Manahoz (S6), and Solaklı (S7), respectively. The Pearson correlation coefficients shown in a half matrix (Table 7) were the results of statistical analyses for the expected relationships between the same water-quality indicators monitored for each stream.

Table 6. Basic statistics of the water-quality indicators monitored in the Eastern Black Sea Basin streams, Turkey (S1: Foldere, S2: Kalenima, S3: Degirmendere, S4: Yomra, S5: Karadere, S6: Manahoz, and S7: Solaklı).

Stations	Water-Quality Indicators (One-year period from March 2015 to February 2016) [81]																							
	WT, °C				pH				LDO, mg/L				LDO Saturation, %				TDS, mg/L				EC, µS/cm			
	Min	Mean	Max	SD	Min	Mean	Max	SD	Min	Mean	Max	SD	Min	Mean	Max	SD	Min	Mean	Max	SD	Min	Mean	Max	SD
S1	2.12	13.74	27.33	7.22	8.14	8.37	9.19	0.30	8.62	11.08	14.48	1.60	99.82	104.21	113.70	4.22	67.74	104.39	164.55	37.16	105.28	178.16	352.47	92.57
S2	0.93	14.58	27.03	7.68	8.31	8.56	9.12	0.26	9.03	10.89	14.45	1.49	97.63	104.79	130.76	9.52	108.65	157.21	211.67	38.81	168.03	265.25	424.53	98.00
S3	3.79	12.89	21.20	5.46	8.33	8.48	8.63	0.10	9.08	11.16	13.54	1.18	98.68	103.91	120.68	5.71	60.55	107.47	159.35	33.21	94.92	172.40	280.60	58.94
S4	3.14	14.72	26.05	7.09	8.09	8.54	9.50	0.40	8.25	10.43	13.53	1.60	97.46	100.18	102.79	1.84	50.11	78.56	134.68	25.06	87.21	136.03	268.93	61.75
S5	3.09	13.66	24.09	6.91	8.08	8.39	8.86	0.27	8.91	11.19	15.08	1.65	98.26	105.25	122.74	6.62	44.97	113.02	420.07	101.86	68.78	194.80	792.53	201.36
S6	3.30	13.45	23.70	6.64	7.74	8.21	8.98	0.40	8.98	11.16	13.97	1.38	98.74	104.79	117.93	5.57	36.03	54.67	82.58	14.72	55.71	91.48	157.87	34.82
S7	3.39	12.70	22.21	5.86	7.74	8.30	8.71	0.27	9.42	11.14	14.00	1.33	96.14	102.91	110.03	3.89	41.01	71.22	97.70	17.86	67.85	115.31	184.05	37.43
Stations	Water-Quality Indicators (One-year period from September 2015 to August 2016)																							
	WT, °C				pH				LDO, mg/L				LDO Saturation, %				TDS, mg/L				EC, µS/cm			
	Min	Mean	Max	SD	Min	Mean	Max	SD	Min	Mean	Max	SD	Min	Mean	Max	SD	Min	Mean	Max	SD	Min	Mean	Max	SD
S1	2.12	13.74	27.35	7.22	7.65	8.29	8.29	0.47	9.64	11.32	14.48	1.41	101.39	106.90	130.44	8.09	39.59	97.44	164.55	37.44	65.42	165.18	317.00	85.74
S2	0.93	14.67	26.81	7.72	7.94	8.49	8.49	0.32	8.84	11.01	14.45	1.47	99.97	105.95	130.76	8.56	50.70	149.90	211.67	46.08	83.43	253.67	424.53	104.53
S3	3.79	13.27	21.20	5.79	7.96	8.39	8.39	0.26	9.07	11.16	13.54	1.33	100.43	104.54	120.68	5.40	60.55	107.47	159.35	31.10	96.35	174.44	280.60	57.84
S4	3.14	14.48	26.05	7.06	7.69	8.56	8.56	0.59	8.25	10.65	13.53	1.58	99.39	101.71	102.89	1.79	56.63	75.16	134.68	23.38	87.21	128.90	268.93	56.61
S5	3.09	13.37	24.09	6.77	7.76	8.34	8.34	0.36	9.70	11.45	15.08	1.63	100.41	106.92	122.74	6.01	57.87	110.25	420.07	100.03	69.60	187.82	792.53	195.86
S6	3.30	13.14	22.53	6.39	7.41	7.98	7.98	0.39	8.98	11.27	13.97	1.44	100.91	104.93	115.03	4.23	39.83	55.40	82.58	14.98	56.76	91.94	157.87	34.14
S7	3.39	12.55	20.20	5.95	7.62	8.19	8.19	0.30	9.56	11.33	14.00	1.43	100.99	104.23	110.03	2.85	38.54	69.06	97.70	16.25	58.11	111.50	184.05	34.97

Table 7. Interstational correlation matrices for water-quality indicators monitored in the Eastern Black Sea Basin streams, Turkey (highlighted cells show the correlation being significant at the 0.01 level).

Stations	Water Temperature, °C						pH					
	S2	S3	S4	S5	S6	S7	S2	S3	S4	S5	S6	S7
S1	0.989 ^b 0.000	0.944 ^b 0.000	0.949 ^b 0.000	0.922 ^b 0.000	0.948 ^b 0.000	0.913 ^b 0.000	0.824 ^b 0.000	0.219 0.383	0.300 0.227	0.309 0.211	0.725 ^b 0.001	0.472 ^a 0.048
S2		0.954 ^b 0.000	0.970 ^b 0.000	0.935 ^b 0.000	0.951 ^b 0.000	0.920 ^b 0.000	–	0.003 0.990	0.584 ^a 0.011	0.202 0.421	0.542 ^a 0.020	0.346 0.159
S3			0.961 ^b 0.000	0.979 ^b 0.000	0.980 ^b 0.000	0.970 ^b 0.000		–	0.121 0.633	0.550 ^a 0.018	0.498 ^a 0.035	0.556 ^a 0.014
S4				0.971 ^b 0.000	0.973 ^b 0.000	0.935 ^b 0.000				0.117 0.643	0.130 0.608	0.165 0.513
S5					0.992 ^b 0.000	0.986 ^b 0.000					0.432 0.074	0.758 ^b 0.000
S6						0.981 ^b 0.000						0.500 ^a 0.035
Stations	Luminescent dissolved oxygen, mg/L						Luminescent dissolved oxygen, %					
	S2	S3	S4	S5	S6	S7	S2	S3	S4	S5	S6	S7
S1	0.935 ^b 0.000	0.883 ^b 0.000	0.933 ^b 0.000	0.933 ^b 0.000	0.911 ^b 0.000	0.896 ^b 0.000	0.588 ^a 0.010	0.206 0.411	0.289 0.245	0.433 0.073	0.695 ^b 0.001	0.689 ^b 0.002
S2		0.894 ^b 0.000	0.914 ^b 0.000	0.885 ^b 0.000	0.863 ^b 0.000	0.837 ^b 0.000		0.716 ^b 0.001	0.312 0.208	0.441 0.067	0.612 ^b 0.007	0.736 ^b 0.000
S3			0.882 ^b 0.000	0.922 ^b 0.000	0.906 ^b 0.000	0.937 ^b 0.000			0.307 0.215	0.338 0.170	0.205 0.414	0.527 ^a 0.025
S4				0.891 ^b 0.000	0.908 ^b 0.000	0.873 ^b 0.000				0.286 0.250	0.178 0.480	0.428 0.077
S5					0.839 ^b 0.000	0.967 ^b 0.000					0.340 0.167	0.650 ^b 0.004
S6						0.968 ^b 0.000						0.812 ^b 0.000
Stations	Total dissolved solids, mg/L						Electrical conductivity, µS/cm					
	S2	S3	S4	S5	S6	S7	S2	S3	S4	S5	S6	S7
S1	0.882 ^b 0.000	0.670 ^b 0.002	0.875 ^b 0.000	0.595 ^b 0.009	0.624 ^b 0.006	0.610 ^b 0.007	0.964 ^b 0.000	0.791 ^b 0.000	0.941 ^b 0.000	0.658 ^b 0.003	0.791 ^b 0.000	0.765 ^b 0.000
S2		0.755 ^b 0.000	0.745 ^b 0.000	0.405 0.095	0.435 0.071	0.579 ^a 0.012		0.788 ^b 0.000	0.887 ^b 0.000	0.578 ^a 0.012	0.672 ^b 0.002	0.689 ^b 0.002
S3			0.601 ^b 0.008	0.536 ^a 0.022	0.623 ^b 0.006	0.910 ^b 0.000			0.749 ^b 0.000	0.707 ^b 0.001	0.731 ^b 0.001	0.907 ^b 0.000
S4				0.798 ^b 0.000	0.767 ^b 0.000	0.602 ^b 0.008				0.816 ^b 0.000	0.855 ^b 0.000	0.762 ^b 0.000
S5					0.741 ^b 0.000	0.662 ^b 0.003					0.777 ^b 0.000	0.782 ^b 0.000
S6						0.740 ^b 0.000						0.856 ^b 0.000

Note: Cells show the Pearson correlation coefficient and the corresponding *P* values. ^a correlation is significant at the 0.05 level (two-tailed); ^b correlation is significant at the 0.01 level (two-tailed).

3.1.1. Flow Rate

The flow rates from the stream gauging stations are presented in the form of time series in Figure 2. Considering the daily mean values for the days when the stream water monitoring was conducted, the flow rates for each stream fluctuated as follows:

0.275 to 17.900 m³/s for the Şerifli (Foldere Stream), 2.170 to 42.300 m³/s for the Öğütlü (Değirmendere Stream), 0.242 to 10.600 m³/s for the Taşdelen (Yomra Stream), 1.840 to 40.800 m³/s for the Ağnas (Karadere Stream).

Taking into account drainage area for each stream gauging station, the flow rate per unit area was calculated as 29.6 L/s/km² for the Foldere, 23.2 L/s/km² for the Değirmendere, 35.4 L/s/km² for the Yomra, and 23.4 L/s/km² for the Karadere.

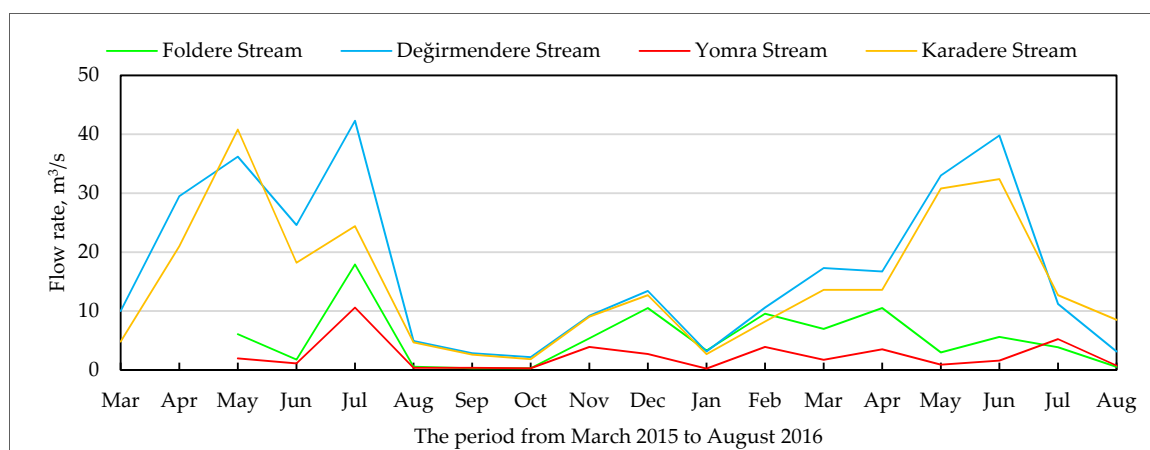


Figure 2. Temporal variation of the stream flow rate during the study period.

3.1.2. Water Temperature

As would be expected, the maximum and minimum values of the stream WT were measured on 1 August 2015, and 3 January 2016, respectively, for each stream, and the vast majority of the stream WT measurements fell within the range of 5.00 to 25.00 °C, throughout the monitoring. On a stream basis, the Solaklı had a relatively lower WT of 12.55 °C, while the Kalenima had a relatively higher WT of 14.67 °C, considering the annual mean values for the last 12 months from September 2015 to August 2016 (Table 6).

On comparing the average air temperature data records between 1981 and 2010 in the weather station (39°45'40" E and 40°59'55" N) of the Turkish State Meteorological Service in the Trabzon Province, the seasonal trend can be given in increasing order, as follows [27]:

7.87 °C in winter < 12.03 °C in spring < 16.40 °C in autumn < 21.43 °C in summer

On a seasonal basis, the same order was being expected as a matter of course for each stream because the temperature of surface waters is naturally determined according to the climate. As would be expected, all streams showed the same trend in that winter presented the coldest stream WT ranging from 6.33 to 7.53 °C, while summer presented the warmest WT values, ranging from 17.98 to 20.49 °C. Interstational correlation coefficients from 0.913 to 0.992 (Table 7) revealed the aforementioned trend.

Based on semimonthly stream WT data records from January 2014 to December 2014, Satilmis [76] reported the seasonal trend for the Değirmendere Stream, in increasing order, as follows:

9.60 °C in winter < 14.24 °C in spring < 16.03 °C in autumn < 24.21 °C in summer

In this study, the seasonal trend, which was the same as that reported by Satilmis [76], for the Değirmendere Stream, were as follows:

7.53 °C in winter < 9.50 °C in spring < 17.64 °C in autumn < 18.41 °C in summer

No classification for the stream WT was available in the TSWQR [75] but a classification was available in the TSWQR [73]. Based on the annual mean values from 12.70 to 14.72 °C for the first 12 months, and from 12.55 to 14.67 °C for the last 12 months, the waters of the EBS basin streams were classified as high quality [73]. Only for the Değirmendere Stream, where the annual mean values were calculated as 12.89 °C for the first 12 months and 13.27 °C for the last 12 months, Satilmis [76] reported a little higher values of WT, with an annual mean value of 16.02 °C and classified the Değirmendere Stream as high quality [73], too.

3.1.3. pH

The vast majority of the stream water pH measurements fell within the range of 7.50 to 9.00, and the values greater than 9.00 were rarely monitored. On a stream basis, Yomra had a relatively higher water pH of 8.53, while Manahoz had a relatively lower water pH of 8.11.

On a seasonal basis, there was no distinct trend in terms of water pH, contrary to the similar trends observed in the WTs, LDO concentrations, and conductivities of the EBS basin streams. Interstational correlation coefficients, which were rarely significant at the 0.01 level (Table 7), revealed this reality.

With reference to the pH range of 6.0–9.0 [75], the waters of the EBS basin streams were classified as high quality. Only for the Değirmendere Stream, where the annual mean values were calculated as 8.48 for the first 12 months and 8.39 for the last 12 months, Satilmis [76] reported similar values of pH, with an annual mean value of 8.35, and also classified the Değirmendere Stream as high quality, too.

3.1.4. Luminescent Dissolved Oxygen Concentration

The vast majority of the stream water LDO measurements fell within the range of 9.00 to 13.00 mg/L, throughout the study, and the values greater than 13.00 mg/L were only monitored on 3 January 2017, when the stream water measurements were in the range of 0.93 to 3.79 °C. On a stream basis, Karadere had a relatively higher LDO concentration of 11.19 mg/L, while Yomra had a relatively lower LDO concentration of 10.43 mg/L, based on the annual mean values for the first 12 months.

On a seasonal basis, all streams showed the same trend, in that, the winter presented the coldest stream temperatures brought about by higher LDO concentrations that varied from 12.31 to 13.26 mg/L, while the summer presented the warmest WT values, which gave rise to lower LDO concentrations that varied from 9.13 to 10.12 mg/L. Interstational correlation coefficients up to $R = 0.968$ (Table 7) revealed the aforementioned trend.

Based on semimonthly LDO data records from January 2014 to December 2014, Satilmis [76] reported the seasonal trend for the Değirmendere Stream, in increasing order, as follows:

8.68 mg/L in summer < 10.17 mg/L in autumn < 10.46 mg/L in spring < 11.19 mg/L in winter.

In this study, the seasonal trend (which was the same as that reported by Satilmis [76]) for the Değirmendere Stream were as follows:

9.63 mg/L in summer < 10.55 mg/L in autumn < 12.03 mg/L in spring < 12.44 mg/L in winter.

Based on the average LDO concentrations from 10.43 to 11.14 mg/L, the waters of the EBS basin streams were classified as high quality [75]. Only for the Değirmendere Stream, where the annual mean values were calculated to be 11.16 mg/L for the first 12 months and 11.16 mg/L for the last 12 months, Satilmis [76] reported a little lower concentration of LDO, with an annual mean value of 10.18 mg/L, and also classified the Değirmendere Stream as high quality.

3.1.5. Luminescent Dissolved Oxygen Saturation

The stream water LDO saturation values were generally greater than 100%. On a stream basis, Karadere had a relatively higher LDO saturation of 105.25%, while Yomra had a relatively lower LDO saturation of 100.18%, based on the annual mean values for the first 12 months.

As such in the stream water LDO concentration, there was no definite seasonal trend in the stream water LDO saturation, since higher values were monitored during summer for the Foldere, Yomra, and Manahoz streams, but during autumn values were monitored for the Kalenima, Değirmendere, Karadere, and Solaklı streams. Nevertheless, it was clear that the springtime LDO saturation values were relatively lower.

No classification for the stream water LDO saturation was available in the TSWQR [75] but a classification was available in the TSWQR [73]. Based on the annual mean values from 100.18% to 105.25% for the first 12 months and 101.71% to 106.92% for the last 12 months, the waters of the EBS basin streams could be classified as high quality [73]. Only for the Değirmendere Stream, where the annual mean values were calculated to be 103.91% for the first 12 months and 104.54% for the last 12 months, Satilmis [76] reported a little lower saturation of LDO, with an annual mean value of 101.42%, and also classified the Değirmendere Stream as high quality.

3.1.6. Total Dissolved Solids

The vast majority of the stream water TDS measurements were lower than 200 mg/L. On a stream basis, the Kalenima Stream had a higher TDS value of 157.21 mg/L, while the Manahoz Stream had a lower EC value of 54.67 mg/L, based on the annual mean values for the first 12 months. On a seasonal basis, all streams, except for the Kalenima and the Değirmendere, showed the same trend, in that, autumn presented higher TDS concentrations, while spring presented lower TDS concentrations. It was thought that lower TDS concentrations were due to higher flow rates. In other words, higher TDS concentrations were due to lower flow rates. The Pearson correlation analysis revealed that the stream TDS concentration was negatively but strongly correlated with the stream flow rate in the Değirmendere and the Yomra ($R = -0.858$ and -0.640 , respectively). The stream TDS concentration was also negatively but moderately correlated with the stream flow rate in the Foldere and the Karadere ($R = -0.606$ and -0.430 , respectively).

As stated by Bayram [11], no classification for TDS is available in the TSWQR [75]. No health-based guideline value is proposed for TDS nationally [77] and internationally [78,79], except for the US EPA [80], in which the allowable concentration is 500 mg/L.

3.1.7. Electrical Conductivity

The vast majority of the stream water EC measurements were lower than 400 $\mu\text{S}/\text{cm}$, which was only exceeded three times in the Kalenima Stream during the period August–October 2016 and one time during August 2016 in the Karadere Stream. As such, in the stream TDS concentration, the Kalenima Stream had a higher EC value of 265.25 $\mu\text{S}/\text{cm}$, while the Manahoz Stream had a lower EC value of 91.48 $\mu\text{S}/\text{cm}$, based on the annual mean values for the first 12 months. As in the stream TDS concentration, it was also thought that the lower EC values were due to higher flow rates. In other words, higher EC values were due to lower flow rates. The Pearson correlation analysis revealed that the stream EC value was negatively but strongly correlated with the stream flow rate in the Değirmendere and the Foldere ($R = -0.831$ and -0.625 , respectively). The stream EC value was also negatively but moderately correlated with the stream flow rate in the Yomra and the Karadere ($R = -0.527$ and -0.412 , respectively).

On a seasonal basis, all streams showed the same trend, in that, autumns that presented higher TDS concentrations brought about higher EC values from 122.26 to 375.12 $\mu\text{S}/\text{cm}$, while springs that presented lower TDS concentrations gave rise to lower EC values from 60.66 to 200.39 $\mu\text{S}/\text{cm}$. Interstitial correlation coefficients up to 0.964 (Table 7) revealed the aforementioned trend.

With reference to the upper threshold value of 400 $\mu\text{S}/\text{cm}$ for EC [75], the waters of the EBS basin streams were classified as high quality. Moreover, the permissible EC value was 2500 $\mu\text{S}/\text{cm}$ at 20 °C, according to TS 266 [77]. The whole measurement results were well below the threshold value. Only for the Değirmendere Stream, where the annual mean values were calculated as 172.40 $\mu\text{S}/\text{cm}$ for the first 12 months and 174.44 $\mu\text{S}/\text{cm}$ for the last 12 months, Satilmis [76] reported similar conductivity values, with an annual mean SC value of 212.26 $\mu\text{S}/\text{cm}$, corresponding to an EC value of 176.53 $\mu\text{S}/\text{cm}$, calculated by using the stream WT and SC data, and also classified the Değirmendere Stream as high quality.

3.2. Stream Water-Quality Modeling

3.2.1. MARS Modeling Results

In this part of the study, a model developed with training data using the stream WT, EC, and pH as the inputs, and the stream LDO concentration as the output. The data from the streams Değirmendere and Manahoz were used to test the developed model. When modeling with the MARS method, it should be noted that the model was influenced by various parameters such as the number of basic functions, the maximum degree of self-interaction, and penalty per knot, etc. These parameters were determined by trial and error. The predicted coefficients and basic functions for the best model were recorded and presented in Table 8 for all models.

Table 8. Basic functions and equations for the multivariate adaptive regression splines (MARS) models.

MARS Model 1		MARS Model 2		MARS Model 3		MARS Model 4	
Basic	Equations	Basic	Equations	Basic	Equations	Basic	Equations
Functions		Functions		Functions		Functions	
BF02	max (0.501816 – WT)	BF02	max (0.501816 – WT)	BF01	max (WT – 0.501816)	BF01	max (WT – 0.501816)
BF03	max (WT – 0.890111)	BF04	max (0.315742 – WT)	BF02	max (0.501816 – WT)	BF02	max (0.501816 – WT)
BF04	max (0.890111 – WT)	BF06	max (0.595661 – WT)	BF03	max (pH – 0.724264) × BF01	BF03	max (pH – 0.724264) × BF01
BF06	max (0.326452 – WT)	BF08	max (0.463269 – WT)	BF05	max (pH – 0.613074) × BF01	BF04	max (0.724264 – pH) × BF01
BF08	max (0.595661 – WT)	BF10	max (0.441271 – WT)	BF07	max (pH – 0.500589) × BF02	BF05	max (pH – 0.613074) × BF01
BF09	max (WT – 0.16559)	BF12	max (0.762159 – WT)	BF09	max (pH – 0.70212) × BF01	BF07	max (pH – 0.500589) × BF02
BF10	max (0.16559 – WT)	BF13	max (WT – 0.828759)	BF11	max (pH – 0.538634) × BF01	BF08	max (0.500589 – pH) × BF02
BF11	max (WT – 0.828759)	BF14	max (0.828759 – WT)	BF12	max (0.538634 – PH) × BF01	BF09	max (pH – 0.70212) × BF01
BF14	max (0.79445 – WT)	BF16	max (0.791625 – WT)	BF13	max (pH – 0.590224) × BF01	BF11	max (pH – 0.538634) × BF01
BF16	max (0.860646 – WT)	BF18	max (0.677397 – WT)	BF15	max (pH – 0.600353) × BF01	BF13	max (pH – 0.590224) × BF01
BF18	max (0.801312 – WT)	BF19	max (WT – 0.284057)	BF17	max (WT – 0.321796)	BF15	max (pH – 0.600353) × BF01
BF20	max (0.791625 – WT)	BF20	max (0.284057 – WT)	BF18	max (0.321796 – WT)	BF17	max (WT – 0.321796)
BF22	max (0.466095 – WT)	BF21	max (WT – 0.374672)	BF19	max (pH – 0.581743) × BF18	BF18	max (0.321796 – WT)
BF24	max (0.340767 – WT)	BF24	max (0.650151 – WT)	BF20	max (0.581743 – pH) × BF18	BF19	max (pH – 0.581743) × BF18
BF26	max (0.671342 – WT)	BF26	max (0.622906 – WT)	BF25	max (pH – 0.175147) × BF17	BF20	max (0.581743 – pH) × BF18
BF28	max (0.444299 – WT)	BF28	max (0.694753 – WT)			BF21	max (pH – 0.437102) × BF01
BF30	max (0.431181 – WT)	BF30	max (0.716347 – WT)			BF33	max (pH – 0.551355) × BF01
BF34	max (0.650151 – WT)	BF31	max (WT – 0.417053)				
BF36	max (0.630575 – WT)	BF32	max (0.417053 – WT)				
BF38	max (0.615439 – WT)	BF34	max (0.340767 – WT)				
BF40	max (0.683451 – WT)	BF36	max (0.55449 – WT)				
		BF38	max (EC – 0.252423)				
		BF39	max (0.252423 – EC)				
LDO _{Model 1} =	0.254679 + 0.0886742 × BF02 + 2.15867 × BF03 + 0.0444198 × BF04 + 0.165892 × BF06 + 0.0705814 × BF08 – 0.0450666 × BF09 – 0.0228572 × BF10 – 0.257149 × BF11 + 0.0483375 × BF14 + 0.0454513 × BF16 + 0.0475508 × BF18 + 0.0485729 × BF20 + 0.0990403 × BF22 + 0.148585 × BF24 + 0.0579245 × BF26 + 0.103979 × BF28 + 0.108156 × BF30 + 0.0612519 × BF34 + 0.0641136 × BF36 + 0.0669608 × BF38 + 0.0565882 × BF40						
LDO _{Model 2} =	0.284243 + 0.0871611 × BF02 + 0.161665 × BF04 + 0.0680995 × BF06 + 0.0992744 × BF08 + 0.104501 × BF10 + 0.0476524 × BF12 – 0.162201 × BF13 + 0.0423067 × BF14 + 0.0453071 × BF16 + 0.0542304 × BF18 – 0.0407528 × BF19 + 0.177219 × BF20 – 0.0414545 × BF21 + 0.0584495 × BF24 + 0.0628739 × BF26 + 0.0526291 × BF28 + 0.0508015 × BF30 – 0.0426374 × BF31 + 0.111746 × BF32 + 0.141249 × BF34 + 0.0754296 × BF36 + 0.0194781 × BF38 + 0.065239 × BF39						
LDO _{Model 3} =	0.433206 + 0.534022 × BF02 – 5.03225 × BF03 + 1.63042 × BF05 + 2.18339 × BF07 + 2.44452 × BF20 – 0.46187 × BF25 – 3.45894 × BF09 – 0.166635 × BF11 – 1.8866 × BF12 + 1.39271 × BF13 + 1.48764 × BF15 – 0.263369 × BF17 + 0.474985 × BF18 + 24.5231 × BF19						
LDO _{Model 4} =	0.31183 – 1.13213 × BF01 + 1.2448 × BF02 + 4.33683 × BF03 + 0.730011 × BF04 + 22.2679 × BF05 + 0.783317 × BF07 + 0.3346 × BF08 – 19.1624 × BF09 – 33.0927 × BF11 + 41.9666 × BF13 – 47.8018 × BF15 + 0.253183 × BF17 + 29.2467 × BF19 + 0.706642 × BF20 + 6.09 × BF21 + 19.8123 × BF23						

The MARS models predicting the LDO concentration involved a total of 21 basic functions for the first one, 23 basic functions for the second one, 15 basic functions for the third one, and 17 basic functions for the last one. The MARS equation for the LDO concentration, which was a function of WT, EC, and pH, could be generated considering Table 8.

3.2.2. TLBO Algorithm and CRA Modeling Results

In this part of the study, the aim was to predict the LDO concentration by employing the TLBO and CRA methods, for all input combinations. Exponential, power, and linear functions were used as a regression function for each method. The best-fit coefficients of the regression functions obtained by the TLBO and CRA methods are given in Table 9, in which the coefficients obtained by each method were very close to each other.

Table 9. Coefficients obtained from the teaching–learning based optimization (TLBO) and conventional regression analysis (CRA) methods.

Models	Methods	Functions	Coefficients				
			w_0	w_1	w_2	w_3	w_4
Model 1	TLBO	$y_{EF}=W_0+exp(W_1+W_2*WT)$	0.0848	0.0683	-2.6255		
	CRA		0.0848	0.0683	-2.6255		
	TLBO	$y_{PF}=W_0*WT^{w_1}$	0.2357	-0.6627			
	CRA		0.2357	-0.6627			
	TLBO	$y_{LF}=W_0+W_1*WT$	0.7912	-0.7633			
	CRA		0.7912	-0.7633			
Model 2	TLBO	$y_{EF}=W_0+exp(W_1+W_2*WT+W_3*EC)$	0.0941	0.0844	-2.6933	-0.0895	
	CRA		0.0938	0.0841	-2.6912	-0.0883	
	TLBO	$y_{PF}=W_0*WT^{w_1}*EC^{w_2}$	0.1681	-0.6621	-0.1991		
	CRA		0.1681	-0.6621	-0.1991		
	TLBO	$y_{LF}=W_0+W_1*WT+W_2*EC$	0.7808	-0.8414	0.2261		
	CRA		0.7808	-0.8414	0.2261		
Model 3	TLBO	$y_{EF}=W_0+exp(W_1+W_2*WT+W_3*pH)$	0.0781	0.0362	-2.5699	0.0697	
	CRA		0.0780	0.0360	-2.5700	-0.0700	
	TLBO	$y_{PF}=W_0*WT^{w_1}*pH^{w_2}$	0.2210	-0.6639	-0.0711		
	CRA		0.2210	-0.6640	-0.0710		
	TLBO	$y_{PF}=W_0*WT^{w_1}*pH^{w_2}$	0.7323	-0.8097	0.1869		
	CRA		0.7320	-0.8100	0.1870		
Model 4	TLBO	$y_{EF}=W_0+exp(W_1+W_2*WT+W_3*EC+W_4*pH)$	0.0886	0.0512	-2.6432	-0.0997	0.0747
	CRA		0.0886	0.0512	-2.6432	-0.0997	0.0747
	TLBO	$y_{PF}=W_0*WT^{w_1}*EC^{w_2}*pH^{w_3}$	0.1695	-0.6606	-0.2135	0.0351	
	CRA		0.1695	-0.6605	-0.2135	0.0351	
	TLBO	$y_{LF}=W_0+W_1*WT+W_2*EC+W_3*pH$	0.7365	-0.8600	0.1737	0.1481	
	CRA		0.7365	-0.8600	0.1737	0.1481	

3.2.3. Comparison of the MARS, TLBO, and CRA Modeling Results

The ability of the MARS method to predict LDO concentration was evaluated by comparing the results of the MARS model with those of the TLBO and CRA methods. The comparisons were made using the RMSE, MAE, and NSCE criteria given in Table 10.

As seen in Table 10, the best results for both the training and testing data sets were obtained from the MARS method, for all models. In other words, the MARS method yielded the least RMSE and highest NSCE values for all models, and the least MAE values for the Models 3 and 4. The best results for each data set were also obtained from Model 4. The results showed that the accuracy of predictions increases with the addition of independent variables.

Table 10. The comparison of the performance measures of the models and methods for the training and testing phases.

Models	Methods	Functions	Training			Testing		
			RMSE	MAE	NSCE	RMSE	MAE	NSCE
Model 1	MARS		0.4109	0.3056	0.9111	0.3718	0.2844	0.9033
	TLBO	Exponential	0.4177	0.3038	0.9082	0.3770	0.2834	0.9005
	TLBO	Power	0.5736	0.4460	0.8269	0.4634	0.3840	0.8497
	TLBO	Linear	0.5703	0.4042	0.8289	0.4418	0.3391	0.8634
	CRA	Exponential	0.4177	0.3038	0.9082	0.3770	0.2834	0.9005
	CRA	Power	0.5736	0.4460	0.8269	0.4636	0.3843	0.8496
	CRA	Linear	0.5703	0.4041	0.8289	0.4418	0.3391	0.8634
Model 2	MARS		0.4123	0.3069	0.9106	0.3686	0.2813	0.9049
	TLBO	Exponential	0.4175	0.3051	0.9083	0.3747	0.2805	0.9017
	TLBO	Power	0.5188	0.4110	0.8584	0.4362	0.3563	0.8668
	TLBO	Linear	0.5387	0.3772	0.8473	0.4534	0.3316	0.8561
	CRA	Exponential	0.4175	0.3050	0.9083	0.3748	0.2805	0.9017
	CRA	Power	0.5188	0.4110	0.8584	0.4362	0.3563	0.8669
	CRA	Linear	0.5387	0.3771	0.8473	0.4535	0.3316	0.8560
Model 3	MARS		0.3134	0.2475	0.9483	0.3382	0.2637	0.9199
	TLBO	Exponential	0.4170	0.3059	0.9085	0.3783	0.2884	0.8998
	TLBO	Power	0.5684	0.4375	0.8300	0.4533	0.3774	0.8562
	TLBO	Linear	0.5360	0.3862	0.8488	0.4397	0.3432	0.8647
	CRA	Exponential	0.4170	0.3060	0.9085	0.3787	0.2888	0.8996
	CRA	Power	0.5684	0.4375	0.8300	0.4533	0.3773	0.8562
	CRA	Linear	0.5361	0.3863	0.8488	0.4405	0.3434	0.8642
Model 4	MARS		0.2599	0.2125	0.9645	0.2709	0.2126	0.9487
	TLBO	Exponential	0.4167	0.3068	0.9086	0.3753	0.2845	0.9014
	TLBO	Power	0.5176	0.4135	0.8590	0.4322	0.3540	0.8693
	TLBO	Linear	0.5180	0.3799	0.8588	0.4561	0.3609	0.8544
	CRA	Exponential	0.4167	0.3068	0.9086	0.3753	0.2845	0.9014
	CRA	Power	0.5176	0.4135	0.8590	0.4322	0.3540	0.8693
	CRA	Linear	0.5180	0.3799	0.8588	0.4561	0.3609	0.8544

For the TLBO and CRA methods, the exponential function provided the best results despite the fact that the lowest error values were obtained from the MARS method for all models. Moreover, when the TLBO and CRA methods were compared, it was seen that the results for each method were very close to each other. Contrary to the initial expectations, it was seen that the employment of the stream EC, together with the stream WT as an input variable was of no use, considering that the performance measure values were close to each other for Models 1 and 2.

From the performance measures, the RMSE and MAE values for the MARS method ranged from 0.2599 to 0.4123 mg/L and 0.2125 to 0.3069 mg/L, respectively, for training and 0.2709 to 0.3718 mg/L and 0.2126 to 0.2844 mg/L, respectively, during testing, as seen in Table 10. The NSCE values ranged from 0.9106 to 0.9645 for training and 0.9033 to 0.9487 for testing. These values meant that the performance of the MARS method was satisfactory. The MARS model with three inputs had the best accuracy in the training and testing periods. In the training data set, the RMSE values for Model 4 were approximately 37% lower than the Models 1 and 2, and approximately 24% lower than Model 3, for the MARS method. Generally, the addition of the EC and pH variables as input variables increased the accuracy of predictions for each method. In particular, the contribution of pH to model performance was greater than that of EC. For the training set, the most suitable results for each model are presented in the form of time-series in Figure 3, in which the stream LDO concentrations modeled by the MARS method are shown as compared to the monitored concentrations.

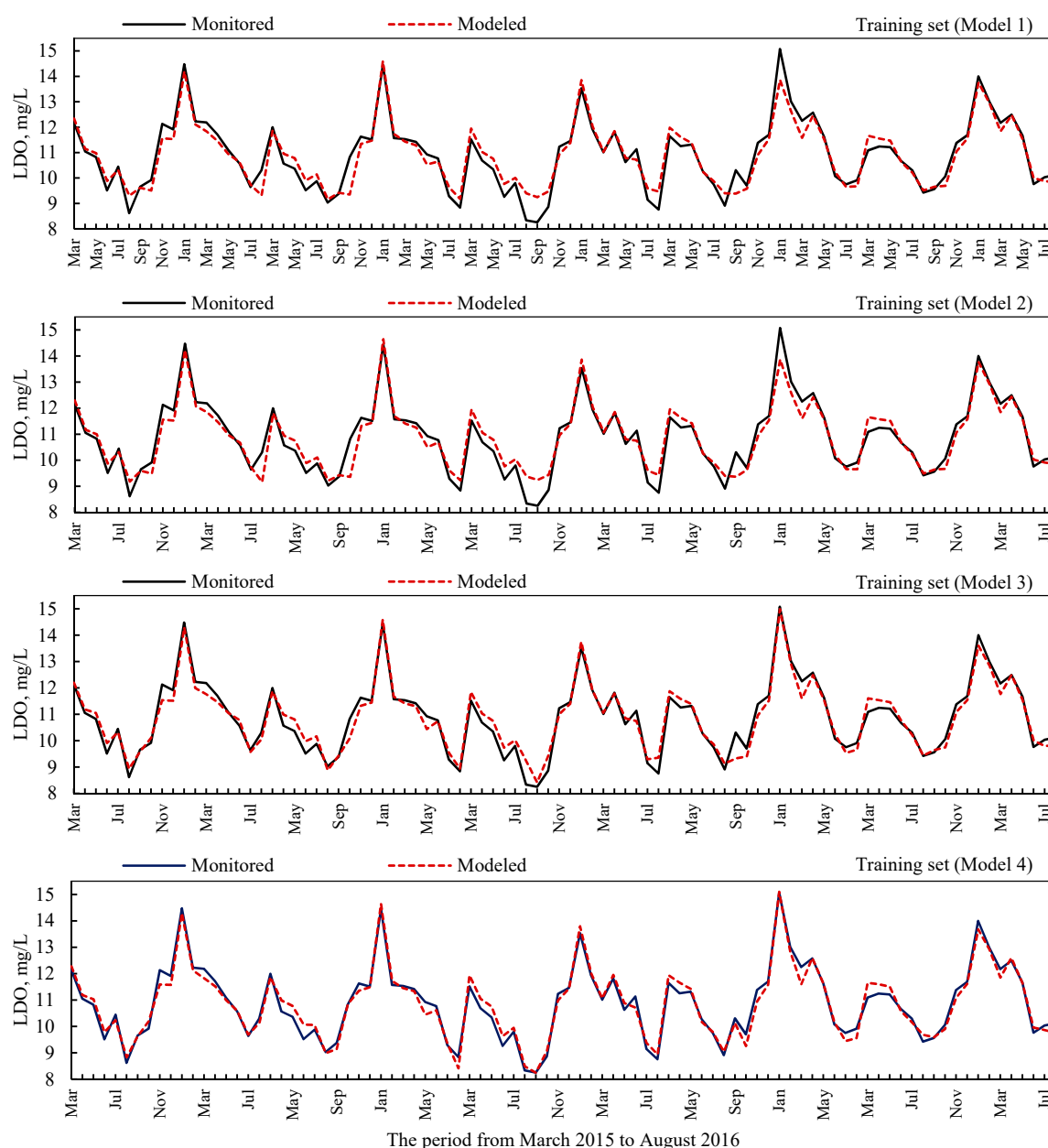


Figure 3. The comparison of the monitored LDO concentrations with the modeled LDO concentrations, employing the MARS method for the training set.

For the testing set, the most suitable results for each model are presented in the form of time series and scatter plots in Figure 4, in which the stream LDO concentrations modeled by the MARS method are shown, as compared to the monitored concentrations.

Figures 3 and 4 show that the stream LDO concentrations modeled by the MARS method for both the training and testing data sets were almost the same as the monitored concentrations. Especially Model 4 gave very satisfactory results at maximum values and minimum values. Additionally, the goodness-of-fit of MARS was evaluated employing R^2 . As shown in Figure 4, there was a high correlation between the monitored and predicted values. The R^2 value in shown in Figure 4 is an indication of a good fit between the monitored and predicted values. This is an important point that demonstrates the success of the MARS method.

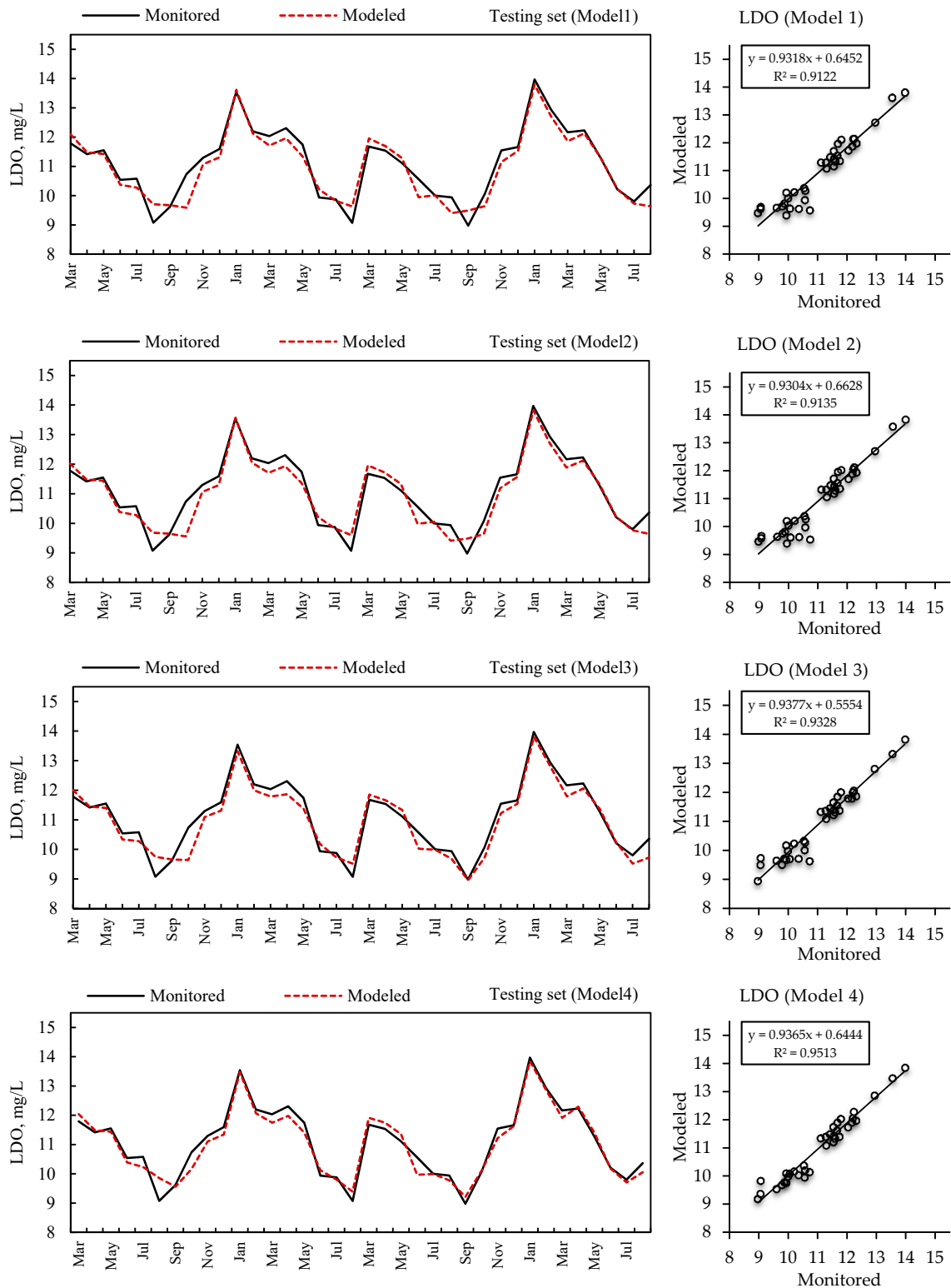


Figure 4. The comparison of the monitored LDO concentrations with the modeled LDO concentrations by employing the MARS method for the testing set.

4. Conclusions

This study consists of two parts. The first, is the monitoring and assessment of the stream water quality in the Eastern Black Sea (EBS) Basin, Turkey, in terms of six water-quality indicators, i.e., water temperature (WT), pH, total dissolved solids (TDS), and electrical conductivity (EC), as well

as luminescent dissolved oxygen (LDO) concentration and saturation. The second one is the spatial forecasting of the stream LDO concentration employing different methods, i.e., multivariate adaptive regression splines (MARS), teaching–learning based optimization (TLBO) algorithm, and conventional regression analysis (CRA), and for different regression functions, i.e., exponential, power, and linear, with different input combination, i.e., WT (Model 1); WT and EC (Model 2); WT and pH (Model 3); WT, EC, and pH (Model 4). In consequence of the monitoring and modeling studies, the following conclusions come into prominence:

- On a seasonal basis, all streams showed the same trend in that the higher LDO concentrations were observed in the winter months with the coldest WT values, while the lower LDO concentrations appeared in the summer months with the warmest WT values. Interstational correlation coefficients up to $R = 0.968$ for the stream LDO concentrations and $R = 0.992$ for the stream WT values supported this trend.
- Autumns, which presented higher TDS concentrations brought about higher EC values, while springs, which presented the lower TDS concentrations gave rise to lower EC values. It was concluded that the higher TDS concentrations were due to the lower flow rates, by taking the negative but strong or moderate correlations into consideration.
- Based on 18-month observations, the waters of the EBS basin streams were classified as high quality, in terms of the monitored water-quality indicators, with reference to the national regulations, being in force in TSWQR [75] and repealed in TSWQR [73].
- The MARS method produced much better results than the TLBO and CRA methods, for both training and testing the data sets for all models, especially for Model 4, which included all input variables.
- The LDO concentrations predicted by the MARS method were almost near the LDO concentrations measured by a portable field meter. It was concluded that the DO concentration could be successfully predicted by the MARS method in any stream, where WT, pH, and EC, or SC were measured but the DO concentration was not monitored, in case of similar watershed characteristics with the studied streams.
- In the TLBO and CRA methods, lower RMSE and MAE, as well as higher NSCE values were obtained by an exponential function for all models. The LDO concentrations predicted by the TLBO method were almost near the LDO concentrations predicted by the CRA method, that is, the TLBO method could not perform any improvement compared to the CRA method.
- It was concluded that the involvement of the pH variable, which is a parameter commonly used for modeling the DO concentration, the independent variables significantly increased the prediction performance.
- Although the history of the MARS method dates back to the pioneering work of Friedman [49], there is a limited availability of its application in the modeling of DO concentration [44,46]. Therefore, the use of this method is encouraged and recommended for studies related to water resources and environment since the proposed MARS method yielded successful results for this study.
- It is expected that the present study will make a significant contribution to the national literature as part of the stream water-quality monitoring and to the international literature as part of the stream water-quality modeling.
- This study will be continued for one and a half year follow up with a monthly frequency, due to limited economic opportunities. For temporal forecasting, a long-term study covering more frequent monitoring is strongly recommended.

Author Contributions: Conceptualization, S.N., and A.B.; Funding acquisition, M.K.; Investigation, S.N., A.B. and O.T.B.; Methodology, S.N., A.B., and M.K.; Supervision, A.B., M.K., and E.A.; Visualization, S.N., and A.B.; Writing—original draft preparation, S.N., and A.B.; Writing—review and editing, S.N., A.B., and M.K. All authors have read and agreed to the published version of the manuscript.

Funding: This research received no external funding.

Acknowledgments: The authors are grateful to Uğur Satılmış (MSc) for their valuable support during the monitoring studies. The authors are also grateful to the providers of the Salford Predictive Modeler 8 software, which was employed to perform the analysis. The staff of the 22nd Regional Directorate of the General Directorate of State Hydraulic Works who are involved in the flow rate measurements are appreciated for their precious contributions. The authors would like to thank the anonymous reviewers for their constructive comments and suggestions that helped to improve the paper.

Conflicts of Interest: The authors declare no conflict of interest.

References

1. Sarkar, A.; Pandey, P. River water quality modelling using artificial neural network technique. *Aquat. Proced.* **2015**, *4*, 1070–1077. [[CrossRef](#)]
2. Cox, B.A. A review of dissolved oxygen modelling techniques for lowland rivers. *Sci. Total Environ.* **2003**, *314*, 303–334. [[CrossRef](#)]
3. Heddam, S. Use of optimally pruned extreme learning machine (OP-ELM) in forecasting dissolved oxygen concentration (DO) Several hours in advance: A case study from the Klamath River, Oregon, USA. *Environ. Process.* **2016**, *3*, 909–937. [[CrossRef](#)]
4. Spanou, M.; Chen, D. An object-oriented tool for the control of point-source pollution in river systems. *Environ. Model. Softw.* **2000**, *15*, 35–54. [[CrossRef](#)]
5. Mulholland, P.J.; Houser, J.N.; Maloney, K.O. Stream diurnal dissolved oxygen profiles as indicators of in-stream metabolism and disturbance effects: Fort Benning as a case study. *Ecol. Indic.* **2005**, *5*, 243–252. [[CrossRef](#)]
6. Sanchez, E.; Colmenarejo, M.F.; Vicente, J.; Rubio, A.; Garcia, M.G.; Travieso, L.; Borja, R. Use of the water quality index and dissolved oxygen deficit as simple indicators of watersheds pollution. *Ecol. Indic.* **2007**, *7*, 315–328. [[CrossRef](#)]
7. Rajwa, A.; Rowinski, P.M.; Bialik, R.J.; Karpinski, M. Stream diurnal profiles of dissolved oxygen-case studies. In Proceedings of the 3rd IAHR Europe Congress, Porto, Portugal, 14–16 April 2014.
8. Lewis, M.E. Dissolved Oxygen, Version 2.0, Chapter A6, Section 6.2. In *Techniques of Water-Resources Investigations, Book 9*; US Geological Survey: Washington, DC, USA, 2006.
9. Bayram, A.; Onsoy, H.; Komurcu, M.I.; Tufekci, M. Reciprocal influence of Kurtun Dam and wastewaters from the settlements on water quality in the stream Harsit, NE Turkey. *Environ. Earth Sci.* **2014**, *72*, 2849–2860. [[CrossRef](#)]
10. Gultekin, F.; Ersoy, A.F.; Hatipoglu, E.; Celep, S. Determination of water quality parameters in wet season of surface water in Trabzon. *Ekoloji* **2012**, *21*, 77–88. [[CrossRef](#)]
11. Bayram, A. Water quality of the Değirmendere stream, drinking water source of Trabzon Province, Turkey. *Desalin. Water Treat.* **2017**, *62*, 120–139. [[CrossRef](#)]
12. Koralay, N.; Kara, O.; Kezik, U. Effects of run-of-the-river hydropower plants on the surface water quality in the Solakli stream watershed, Northeastern Turkey. *Water Environ. J.* **2018**, *32*, 412–421. [[CrossRef](#)]
13. Cox, B.A. A review of currently available in-stream water-quality models and their applicability for simulating dissolved oxygen in lowland rivers. *Sci. Total Environ.* **2003**, *314*, 335–377. [[CrossRef](#)]
14. Rankovic, V.; Radulovic, J.; Radojevic, I.; Ostojic, A.; Comic, L. Neural network modeling of dissolved oxygen in the Gruza reservoir, Serbia. *Ecol. Modell.* **2010**, *221*, 1239–1244. [[CrossRef](#)]
15. Soyupak, S.; Karaer, F.; Gürbüz, H.; Kivrak, E.; Sentürk, E.; Yazici, A. A neural network-based approach for calculating dissolved oxygen profiles in reservoirs. *Neural Comput. Appl.* **2003**, *12*, 166–172. [[CrossRef](#)]
16. Sengorur, B.; Dogan, E.; Koklu, R.; Samandar, A. Dissolved oxygen estimation using artificial neural network for water quality control. *Fresenius Environ. Bull.* **2006**, *15*, 1064–1067.
17. Kanda, E.K.; Kosgei, J.R.; Kipkorir, E.C. Simulation of organic carbon loading using MIKE 11 model: A case of River Nzoia, Kenya. *Water Pract. Technol.* **2015**, *10*, 298–304. [[CrossRef](#)]
18. Najah, A.; El-Shafie, A.; Karim, O.A.; El-Shafie, A.H. Performance of ANFIS versus MLP-NN dissolved oxygen prediction models in water quality monitoring. *Environ. Sci. Pollut. Res.* **2014**, *21*, 1658–1670. [[CrossRef](#)] [[PubMed](#)]
19. Ay, M.; Kisi, O. Estimation of dissolved oxygen by using neural networks and neuro fuzzy computing techniques. *KSCE J. Civ. Eng.* **2017**, *21*, 1631–1639. [[CrossRef](#)]

20. Singh, K.P.; Malik, A.; Mohan, D.; Sinha, S. Multivariate statistical techniques for the evaluation of spatial and temporal variations in water quality of Gomti River (India)—A case study. *Water Res.* **2004**, *38*, 3980–3992. [[CrossRef](#)]
21. Zhang, Q.; Li, Z.; Zeng, G.; Li, J.; Fang, Y.; Yuan, Q.; Wang, Y.; Ye, F. Assessment of surface water quality using multivariate statistical techniques in red soil hilly region: A case study of Xiangjiang watershed, China. *Environ. Monit. Assess.* **2009**, *152*, 123–131. [[CrossRef](#)]
22. Bu, H.; Tan, X.; Li, S.; Zhang, Q. Water quality assessment of the Jinshui River (China) using multivariate statistical techniques. *Environ. Earth Sci.* **2010**, *60*, 1631–1639. [[CrossRef](#)]
23. Panepinto, D.; Genon, G. Modeling of Po River water quality in Torino (Italy). *Water Resour. Manag.* **2010**, *24*, 2937–2958. [[CrossRef](#)]
24. Akbal, F.; Gurel, L.; Bahadir, T.; Guler, I.; Bakan, G.; Buyukgungor, H. Multivariate statistical techniques for the assessment of surface water quality at the mid-black sea coast of Turkey. *Water Air Soil Pollut.* **2011**, *216*, 21–37. [[CrossRef](#)]
25. DSİ. General Directorate of State Hydraulic Works (Devlet Su İşleri Genel Müdürlüğü, in Turkish). DSİ 2016 Yılı Resmi Su Kaynakları İstatistikleri, Havzalara Göre Yıllık Ortalama Yüzeysuyu Su Potansiyeli, 2013–2016. Available online: <http://www.dsi.gov.tr/dsi-resmi-istatistikler/resmi-i-statistikler-2016/2016-y%C4%B1l%C4%B1-verileri> (accessed on 6 March 2020).
26. TÜİK. Turkish Statistical Institute (Türkiye İstatistik Kurumu, in Turkish). Nüfus ve Demografi, Yıllara Göre İl Nüfusları. Available online: <http://tuik.gov.tr/UstMenu.do?metod=temelist> (accessed on 6 March 2020).
27. TÜİK. (Turkish Statistical Institute (Türkiye İstatistik Kurumu, in Turkish)). Municipal population served by the sewerage system. Available online: <https://biruni.tuik.gov.tr/medas/?kn=120&locale=en> (accessed on 6 March 2020).
28. DSİ. General Directorate of State Hydraulic Works (Devlet Su İşleri Genel Müdürlüğü, in Turkish). 2015 Akım Gözlem Yıllığı. Available online: http://www.dsi.gov.tr/docs/agi-y\T1\ill\T1\ik-dsi/dsi_2015.pdf?sfvrsn=2 (accessed on 6 March 2020).
29. Diamantopoulou, M.J.; Antonopoulos, V.Z.; Papamichail, D.M. Cascade correlation artificial neural networks for estimating missing monthly values of water quality parameters in rivers. *Water Resour. Manag.* **2007**, *21*, 649–662. [[CrossRef](#)]
30. Chen, L.H.; Li, L. Evaluation of dissolved oxygen in water by artificial neural network and sample optimization. *J. Cent. South Univ. Technol.* **2008**, *15*, 416–420. [[CrossRef](#)]
31. Singh, K.P.; Basant, A.; Malik, A.; Jain, G. Artificial neural network modeling of the river water quality—A case study. *Ecol. Model.* **2009**, *220*, 888–895. [[CrossRef](#)]
32. Ay, M.; Kisi, O. Modeling of dissolved oxygen concentration using different neural network techniques in Foundation Creek, El Paso County, Colorado. *J. Environ. Eng.* **2011**, *138*, 654–662. [[CrossRef](#)]
33. Wen, X.; Fang, J.; Diao, M.; Zhang, C. Artificial neural network modeling of dissolved oxygen in the Heihe River, Northwestern China. *Environ. Monit. Assess.* **2013**, *185*, 4361–4371. [[CrossRef](#)] [[PubMed](#)]
34. Antanasijevic, D.; Pocajt, V.; Povrenovic, D.; Peric-Grujic, A.; Ristic, M. Modelling of dissolved oxygen content using artificial neural networks: Danube River, North Serbia, case study. *Environ. Sci. Pollut. Res.* **2013**, *20*, 9006–9013. [[CrossRef](#)]
35. Kisi, O.; Akbari, N.; Sanatipour, M.; Hashemi, A.; Teimourzadeh, K.; Shiri, J. Modeling of dissolved oxygen in river water using artificial intelligence techniques. *J. Environ. Inf.* **2013**, *22*, 92–101. [[CrossRef](#)]
36. Heddam, S. Modeling hourly dissolved oxygen concentration (DO) using two different adaptive neuro-fuzzy inference systems (ANFIS): A comparative study. *Environ. Monit. Assess.* **2014**, *186*, 597–619. [[CrossRef](#)]
37. Evrendilek, F.; Karakaya, N. Monitoring diel dissolved oxygen dynamics through integrating wavelet denoising and temporal neural networks. *Environ. Monit. Assess.* **2014**, *186*, 1583–1591. [[CrossRef](#)] [[PubMed](#)]
38. Heddam, S. Generalized regression neural network-based approach for modelling hourly dissolved oxygen concentration in the Upper Klamath River, Oregon, USA. *Environ. Technol.* **2014**, *35*, 1650–1657. [[CrossRef](#)]
39. Heddam, S. Modelling hourly dissolved oxygen concentration (DO) using dynamic evolving neural-fuzzy inference system (DENFIS)-based approach: Case study of Klamath River at Miller Island Boat Ramp, OR, USA. *Environ. Sci. Pollut. Res.* **2014**, *21*, 9212–9227. [[CrossRef](#)] [[PubMed](#)]
40. Nemati, S.; Fazelifard, M.H.; Terzi, O.; Ghorbani, M.A. Estimation of dissolved oxygen using data-driven techniques in the Tai Po River, Hong Kong. *Environ. Earth Sci.* **2015**, *74*, 4065–4073. [[CrossRef](#)]

41. Bayram, A.; Kankal, M. Artificial Neural Network Modeling of Dissolved Oxygen Concentration in a Turkish Watershed. *Pol. J. Environ. Stud.* **2015**, *24*, 1507–1515.
42. Kanda, E.K.; Kipkorir, E.C.; Kosgei, J.R. Dissolved oxygen modelling using artificial neural network: A case of River Nzoia, Lake Victoria basin, Kenya. *J. Water Sec.* **2016**, *2*. [[CrossRef](#)]
43. Olyiaie, E.; Abyaneh, H.Z.; Mehr, A.D. A comparative analysis among computational intelligence techniques for dissolved oxygen prediction in Delaware River. *Geosci. Front.* **2017**, *8*, 517–527. [[CrossRef](#)]
44. Heddami, S.; Kisi, O. Modelling daily dissolved oxygen concentration using least square support vector machine, multivariate adaptive regression splines and M5 model tree. *J. Hydrol.* **2018**, *559*, 499–509. [[CrossRef](#)]
45. Elkiran, G.; Nourani, V.; Abba, S.I.; Abdullahi, J. Artificial intelligence-based approaches for multi-station modelling of dissolved oxygen in river. *Glob. J. Environ. Sci. Manag.* **2018**, *4*, 439–450.
46. Yaseen, Z.M.; Ehteram, M.; Sharafati, A.; Shahid, S.; Al-Ansari, N.; El-Shafie, A. The integration of nature-inspired algorithms with least square support vector regression models: Application to modeling river dissolved oxygen concentration. *Water* **2018**, *10*, 1124. [[CrossRef](#)]
47. Csabragi, A.; Molnar, S.; Tanos, P.; Kovacs, J.; Molnar, M.; Szabo, I.; Hatvani, I.G. Estimation of dissolved oxygen in riverine ecosystems: Comparison of differently optimized neural networks. *Ecol. Eng.* **2019**, *138*, 298–309. [[CrossRef](#)]
48. Kisi, O.; Alizamir, M.; Gorgij, A.D. Dissolved oxygen prediction using a new ensemble method. *Environ. Sci. Pollut. Res.* **2020**, *27*, 9589–9603. [[CrossRef](#)] [[PubMed](#)]
49. Friedman, J.H. Multivariate adaptive regression splines. *Ann. Statist.* **1991**, *19*, 79–141. [[CrossRef](#)]
50. Zhang, W.; Goh, A.T. Multivariate adaptive regression splines and neural network models for prediction of pile drivability. *Geosci. Front.* **2016**, *7*, 45–52. [[CrossRef](#)]
51. Kisi, O.; Parmar, K.S. Application of least square support vector machine and multivariate adaptive regression spline models in long term prediction of river water pollution. *J. Hydrol.* **2016**, *534*, 104–112. [[CrossRef](#)]
52. Tiryaki, S.; Tan, H.; Bardak, S.; Kankal, M.; Nacar, S.; Peker, H. Performance evaluation of multiple adaptive regression splines, teaching–learning based optimization and conventional regression techniques in predicting mechanical properties of impregnated wood. *Eur. J. Wood Wood Prod.* **2019**, *77*, 645–659. [[CrossRef](#)]
53. Suman, S. Prediction of Pile Capacity Parameters Using Functional Networks and Multivariate Adaptive Regression Splines. Master’s Thesis, National Institute of Technology, Odisha, India, 2015.
54. Samui, P. Multivariate adaptive regression spline (Mars) for prediction of elastic modulus of jointed rock mass. *Geotech. Geol. Eng.* **2013**, *31*, 249–253. [[CrossRef](#)]
55. Khuntia, S.; Mujtaba, H.; Patra, C.; Farooq, K.; Sivakugan, N.; Das, B.M. Prediction of compaction parameters of coarse grained soil using multivariate adaptive regression splines (MARS). *Int. J. Geotech. Eng.* **2015**, *9*, 79–88. [[CrossRef](#)]
56. Dey, P.; Das, A.K. Application of multivariate adaptive regression spline-assisted objective function on optimization of heat transfer rate around a cylinder. *Nucl. Eng. Technol.* **2016**, *48*, 1315–1320. [[CrossRef](#)]
57. Rao, R.V.; Savsani, V.J.; Vakharia, D.P. Teaching–learning-based optimization: A novel method for constrained mechanical design optimization problems. *Comput. Aided Des.* **2011**, *43*, 303–315. [[CrossRef](#)]
58. Rao, R.V.; Savsani, V.J.; Vakharia, D.P. Teaching–learning-based optimization: An optimization method for continuous non-linear large scale problems. *Inf. Sci.* **2012**, *183*, 1–15. [[CrossRef](#)]
59. Dede, T. Optimum design of grillage structures to LRFD-AISC with teaching–learning based optimization. *Struct. Multidiscip. Optim.* **2013**, *48*, 955–964. [[CrossRef](#)]
60. Togan, V. Design of pin jointed structures using teaching–learning based optimization. *Struct. Eng. Mech.* **2013**, *47*, 209–225. [[CrossRef](#)]
61. Csabragi, A.; Molnar, S.; Tanos, P.; Kovacs, J. Application of artificial neural networks to the forecasting of dissolved oxygen content in the Hungarian section of the river Danube. *Ecol. Eng.* **2017**, *100*, 63–72. [[CrossRef](#)]
62. Palani, S.; Liong, S.Y.; Tkalich, P. An ANN application for water quality forecasting. *Mar. Pollut. Bull.* **2008**, *56*, 1586–1597. [[CrossRef](#)] [[PubMed](#)]
63. Bayram, A.; Kankal, M.; Onsoy, H. Estimation of suspended sediment concentration from turbidity measurements using artificial neural networks. *Environ. Monit. Assess.* **2012**, *184*, 4355–4365. [[CrossRef](#)]
64. Fetene, B.N.; Shufen, R.; Dixit, U.S. FEM-based neural network modeling of laser-assisted bending. *Neural Comput. Appl.* **2018**, *29*, 69–82. [[CrossRef](#)]

65. Nacar, S.; Hınıs, M.A.; Kankal, M. Forecasting daily streamflow discharges using various neural network models and training algorithms. *KSCE J. Civ. Eng.* **2018**, *22*, 3676–3685. [CrossRef]
66. Dawson, C.W.; Wilby, R. An artificial neural network approach to rainfall-runoff modelling. *Hydrol. Sci. J.* **1998**, *43*, 47–66. [CrossRef]
67. Legates, D.R.; McCabe, G.J. Evaluating the use of “goodness-of-fit” measures in hydrologic and hydroclimatic model validation. *Water Resour. Res.* **1999**, *35*, 233–241. [CrossRef]
68. Uluer, O.; Kirmaci, V.; Atas, S. Using the artificial neural network model for modeling the performance of the counter flow vortex tube. *Expert Syst. Appl.* **2009**, *36*, 12256–12263. [CrossRef]
69. TWPCR. *Turkish Water Pollution Control Regulation*; The Official Gazette No.: 25687; (Su Kirliliği Kontrolü Yönetmeliği, in Turkish); The Official Gazette of the Republic of Turkey: Ankara, Turkey, 2004.
70. Yesilnacar, M.I.; Uyanik, S. Investigation of water quality of the world’s largest irrigation tunnel system, the Sanliurfa tunnels in Turkey. *Fresenius Environ. Bull.* **2005**, *14*, 300–306.
71. Bulut, V.N.; Bayram, A.; Gundogdu, A.; Soylak, M.; Tufekci, M. Assessment of water quality variables in the stream Galyan, Trabzon, Turkey. *Environ. Monit. Assess.* **2010**, *165*, 1–13. [CrossRef] [PubMed]
72. TSWQMR. *Turkish Superficial Water Quality Management Regulation*; The Official Gazette No.: 28483; (Yüzeysel Su Kalitesi Yönetimi Yönetmeliği, in Turkish); The Official Gazette of the Republic of Turkey: Ankara, Turkey, 2012.
73. TSWQR. *Turkish Surface Water Quality Regulation*; The Official Gazette No.: 29327; (Yüzeysel Su Kalitesi Yönetimi Yönetmeliğinde Değişiklik Yapılmasına Dair Yönetmelik, in Turkish); The Official Gazette of the Republic of Turkey: Ankara, Turkey, 2015.
74. Bayram, A. Rebuttal to ‘Evaluation of surface water quality and heavy metal pollution of Coruh River Basin (Turkey) by multivariate statistical methods’ by Bilgin and Konanc (Environ. Earth Sci. **2016**, *75*, 1029). *Environ. Earth Sci.* **2017**, *76*, 700. [CrossRef]
75. TSWQR. *Turkish Surface Water Quality Regulation*; The Official Gazette No.: 29797; (Yerüstü Su Kalitesi Yönetmeliğinde Değişiklik Yapılmasına Dair Yönetmelik, in Turkish); The Official Gazette of the Republic of Turkey: Ankara, Turkey, 2016.
76. Satilmis, U. A Study on Spatial and Temporal Variation of Surface Water Quality in the Stream Değirmendere Watershed (Trabzon). Master’s Thesis, Karadeniz Technical University, Trabzon, Turkey, 2015. (In Turkish with English abstract).
77. TS 266. *Water Intended for Human Consumption*; (Sular-İnsani Tüketim Amaçlı Sular, in Turkish); Türk Standartları Enstitüsü (TSE): Ankara, Turkey, 2005.
78. EU 1998 Official Journal of European Communities, Council Directive 98/83/EC of 3 November 1998 on the Quality of Water Intended for Human Consumption. Available online: <http://eurlex.europa.eu/LexUriServ/LexUriServ.do?uri=OJ:L:1998:330:0032:0054:EN:PDF> (accessed on 29 February 2020).
79. WHO. *Guidelines for Drinking-Water Quality*, 4th ed.; World Health Organization: Geneva, Switzerland, 2011.
80. US EPA. *Drinking Water Standards and Health Advisories*; United States Environmental Protection Agency: Washington, DC, USA, 2009. Available online: <http://water.epa.gov/action/advisories/drinking/upload/dwstandards2009.pdf> (accessed on 29 February 2020).
81. Nacar, S.; Bayram, A.; Satilmis, U.; Baki, O.T. The surface water quality monitoring and assessment of the Eastern Black Sea Basin (Trabzon Province) Streams, Turkey. In Proceedings of the 12th International Congress on Advances in Civil Engineering, İstanbul, Turkey, 21–23 September 2016; Turan, Ö., Hilmi, L., Eds.; p. 111, (Full text in CD).

